Received: 19 July 2023 | Revised: 13 September 2023 | Accepted: 13 October 2023

DOI: 10.1002/ar.25343

SPECIAL ISSUE ARTICLE

The Anatomical Record WILEY

Incongruent ontogenetic maturity indicators in a Late Triassic archosaur (Aetosauria: *Typothorax coccinarum*)

William G. Parker[1] | **William A. Reyes**[1,2] | **Adam D. Marsh**[1]

[1]Department of Science and Resource Management, Petrified Forest National Park, Petrified Forest, USA

[2]Jackson School of Geosciences, University of Texas, Austin, Texas, USA

Correspondence
William G. Parker, Department of Science and Resource Management, Petrified Forest National Park, AZ 86028, USA.
Email: william_parker@nps.gov

Funding information
National Science Foundation Graduate Research Fellowship Program, Grant/Award Number: 2137420

Abstract

Maximum individual body size in pseudosuchian archosaurs is not well constrained in the fossil record, but it may be influenced by a variety of factors including basal metabolic rate, evolutionary relationships, and environmental conditions. Body size varies among the Aetosauria in which estimated total length ranges between 1 m (e.g., *Coahomasuchus kahleorum*) and 5 m (e.g., *Desmatosuchus spurensis*). A new, very large specimen of the aetosaurian *Typothorax coccinarum* from Petrified Forest National Park in northeastern Arizona is nearly twice the size of all other known specimens of *Typothorax* and is the largest aetosaur specimen currently known worldwide. The specimen lacks co-ossified neurocentral sutures in the trunk vertebrae which may suggest that the individual had not yet reached skeletal maturity, yet smaller specimens of *T. coccinarum* exhibit partially or fully co-ossified neurocentral sutures in the same region. If body size correlates with skeletal maturity in aetosaurs, this discrepancy warns that timing of neurocentral suture co-ossification in aetosaurs may not be a reliable indicator of ontogenetic stage. Osteohistological observations of a trunk rib demonstrate that although PEFO 42506 shows a large body size, the specimen did not deposit an external fundamental system despite depositing as many as 19 growth lines, further indicating that it had not yet reached skeletal maturity. Thus, at least within Aetosauria, neurocentral suture co-ossification and skeletal maturity may correlate, whereas body size can be incongruent in comparison. Furthermore, this specimen indicates that non-desmatosuchin aetosaurs could exhibit large body sizes and suggests that some aetosaurs may have experienced indeterminate growth.

KEYWORDS

aetosaur, Chinle Formation, growth, pseudosuchia, size

1 | INTRODUCTION

Aetosaurs are heavily armored pseudosuchian archosaurs known exclusively from terrestrial Upper Triassic strata (Desojo et al., 2013). Aetosaurs are of interest because they are relatively common and taxonomically diverse, but more importantly, they possess diagnostic skeletal elements (i.e., osteoderms) that allow them to be easily identified and useful for vertebrate biostratigraphy (Heckert & Lucas, 2000; Long & Ballew, 1985; Long & Murry, 1995;

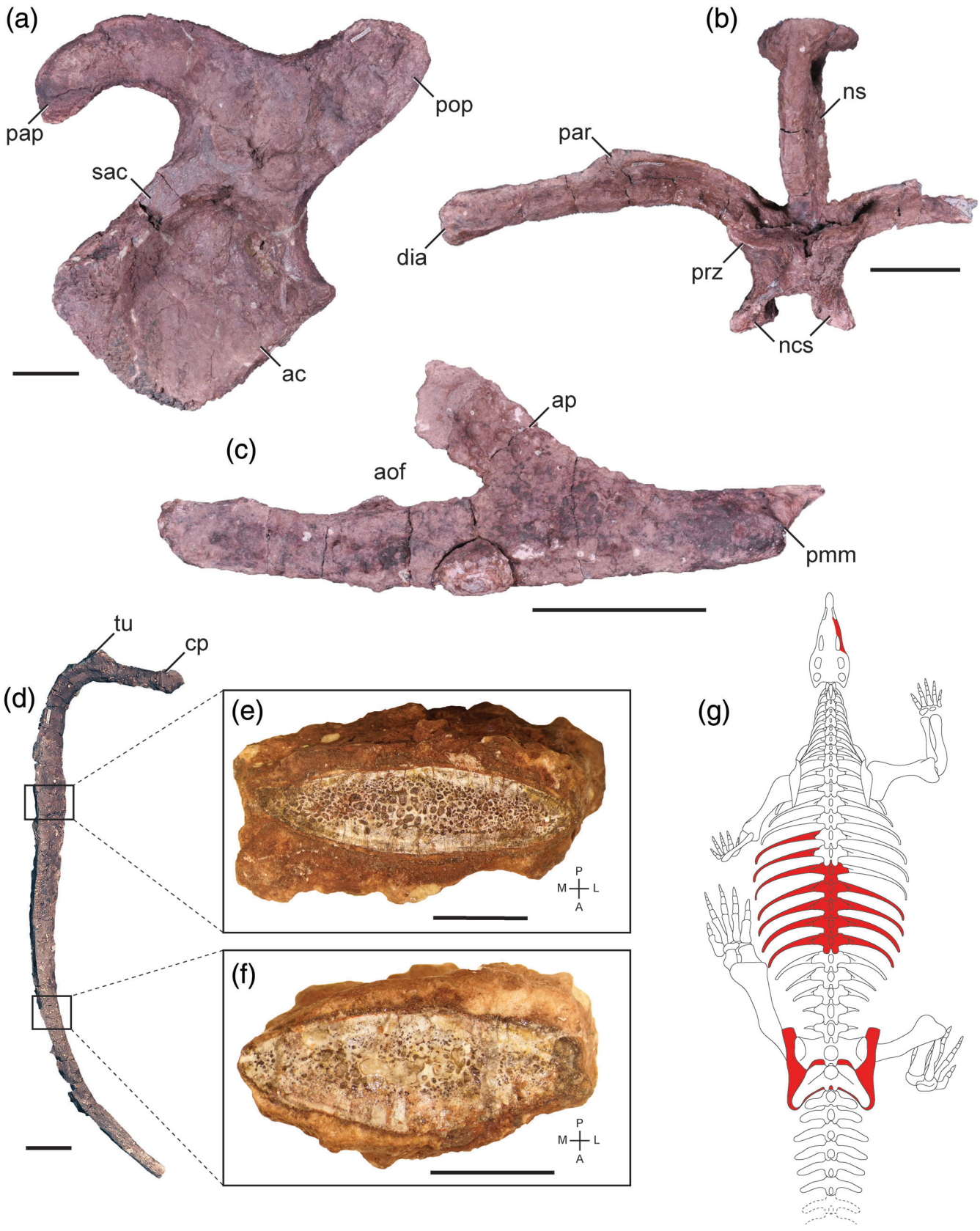

FIGURE 1 Legend on next page.

Lucas & Hunt, 1993). Aetosaurs have a wide range of body sizes from 1 m to nearly 5 m in total length (Desojo et al., 2013). In addition, aetosaurs of similar age and body length can vary in overall mass, reflective of wide versus narrow body shapes (Taborda et al., 2013). The largest aetosaur specimen presently known is MNA V9300, an individual of *Desmatosuchus spurensis* that has an estimated body length of >5 m (Parker, 2008). Desmatosuchins (sensu Parker, 2016) tend to have the largest body sizes among aetosaurs, followed by the relatively wide-bodied typothoracines (Desojo et al., 2013; Heckert & Lucas, 2000; Parker, 2008).

In this contribution, we present a large specimen of the typothoracine *Typothorax coccinarum* (PEFO 42506) from the Petrified Forest Member of the Chinle Formation of Arizona (Figure 1). Currently, this specimen represents the largest reported aetosaur to date (see details below). The size discrepancy between the preserved elements of PEFO 42506 and that of other specimens of *T. coccinarum* (Figure 2) makes it ideal for studying the skeletal growth of this taxon. What is significant about PEFO 42506, aside from its large body size, is that the trunk vertebral centra and associated neural arches are not co-ossified (Figure 1b). Co-ossification of the centrum and neural arch has been used as a proxy for assessing skeletal maturity in some archosaurian groups (Brochu, 1996; Irmis, 2007); the co-ossification of the neurocentral suture occurs in a posterior-to-anterior sequence through ontogeny in *Alligator mississippiensis*, where co-ossified vertebral centra and their respective neural arches indicate that the specimen is skeletally mature and is often associated with larger individuals of a taxon (Griffin et al., 2020). This pattern has been utilized for other archosaurian groups, but the timing and pattern of neurocentral sutures varies between clades (Irmis, 2007) and there is evidence of intraspecific plasticity among some taxa (e.g., *Coelophysis bauri*; Griffin, 2018; Griffin et al., 2020). Irmis (2007) and Griffin et al. (2020) advocated that osteohistology be integrated with skeletal criteria to better determine archosaurian ontogeny. Thus, we assessed the skeletal maturity of PEFO 42506 through histological analysis to test whether large body size and neurocentral suture co-ossification is associated with skeletal maturity in some aetosaurs.

Most previous histological studies on aetosauriforms (i.e., aetosaurs, *Acaenasuchus geoffreyi*, *Revueltosaurus callenderi*; Parker et al., 2008; Scheyer et al., 2014; Marsh et al., 2020; Parker et al., 2021) focused on sampling the dorsal carapace (i.e., paramedian and lateral osteoderms). This is because osteoderms (including fragments) are the most common fossilized elements of the group (Desojo et al., 2013; Long & Ballew, 1985). Appendicular bones of aetosaurs from the *Placerias* Quarry (UCMP A269) of Arizona have been used for histological studies (e.g., de Ricqlès et al., 2003); however, the species-level referrals of those individual elements are ambiguous (Parker, 2018; Reyes et al., 2023). Despite the lack of data obtained from the appendicular region (e.g., de Ricqlès et al., 2003; Teschner et al., 2022, 2023), histological analyses of osteoderms have aided in determining approximate skeletal maturity and growth curves of a few aetosaur taxa (e.g., Cerda et al., 2018; Cerda & Desojo, 2011; de Ricqlès et al., 2021; Hoffman et al., 2019; Paes-Neto et al., 2021; Parker et al., 2008; Scheyer et al., 2014; Taborda et al., 2013; Teschner et al., 2023; Werning, 2013).

Recently, Ponce et al. (2023) sampled osteoderms and associated limb bones from two specimens of differing sizes of *Aetosauroides scagliai*. Significantly, that study showed that discrepancies exist between age estimates based on lines of arrested growth dependent on the element sampled, and those based on size. They concluded that because of differences in timing in bone remodeling between osteoderms and appendicular elements that osteoderms were the best indicator of age in the late stages of growth (Ponce et al., 2023). Strangely, no osteoderms were found with the associated skeleton of PEFO 42506 despite its large body size and the frequency at which aetosaur osteoderms are preserved; only an isolated right maxilla, trunk vertebrae, trunk ribs (primarily from the left side of the body), and partial pelvis were preserved (Figure 1g). Because of the limited elements available, histological analysis of PEFO 42506 was restricted to the trunk ribs.

Histological analyses are often selective toward the shaft of long bones or osteoderms (Lee et al., 2013; Woodward et al., 2013; Griffin et al., 2020; de Buffrénil et al., 2021). However, ribs have also been found to be informative in assessing skeletal maturity in a range of

FIGURE 1 Skeletal elements of *Typothorax coccinarum* (PEFO 42506). (a) left ilium in lateral view; (b), trunk vertebra in anterior view; (c) right maxilla in lateral view; (d–f) left trunk rib in posterior view (d) with dashed lines indicating location of the proximal (e) and distal (f) histological samples (in proximal view); (g) reconstruction of a typothoracine aetosaur with osteoderms removed showing estimated positions of preserved elements (red) of PEFO 42506 (modified from Walker, 1961). a, anterior; aof, antorbital fenestra; ap, ascending process; ca, capitulum; dia, diapophysis; L, lateral; M, medial; ncs, neurocentral suture; ns, neural spine; P, posterior; pap, preacetabular process; par, parapophysis; pmm, premaxilla-maxilla contact; pop, postacetabular process; prz, prezygapophysis; sac, supraacetabular crest; tu, tuberculum. Scale bars equal 5 cm (a–d) and 1 cm (e,f).

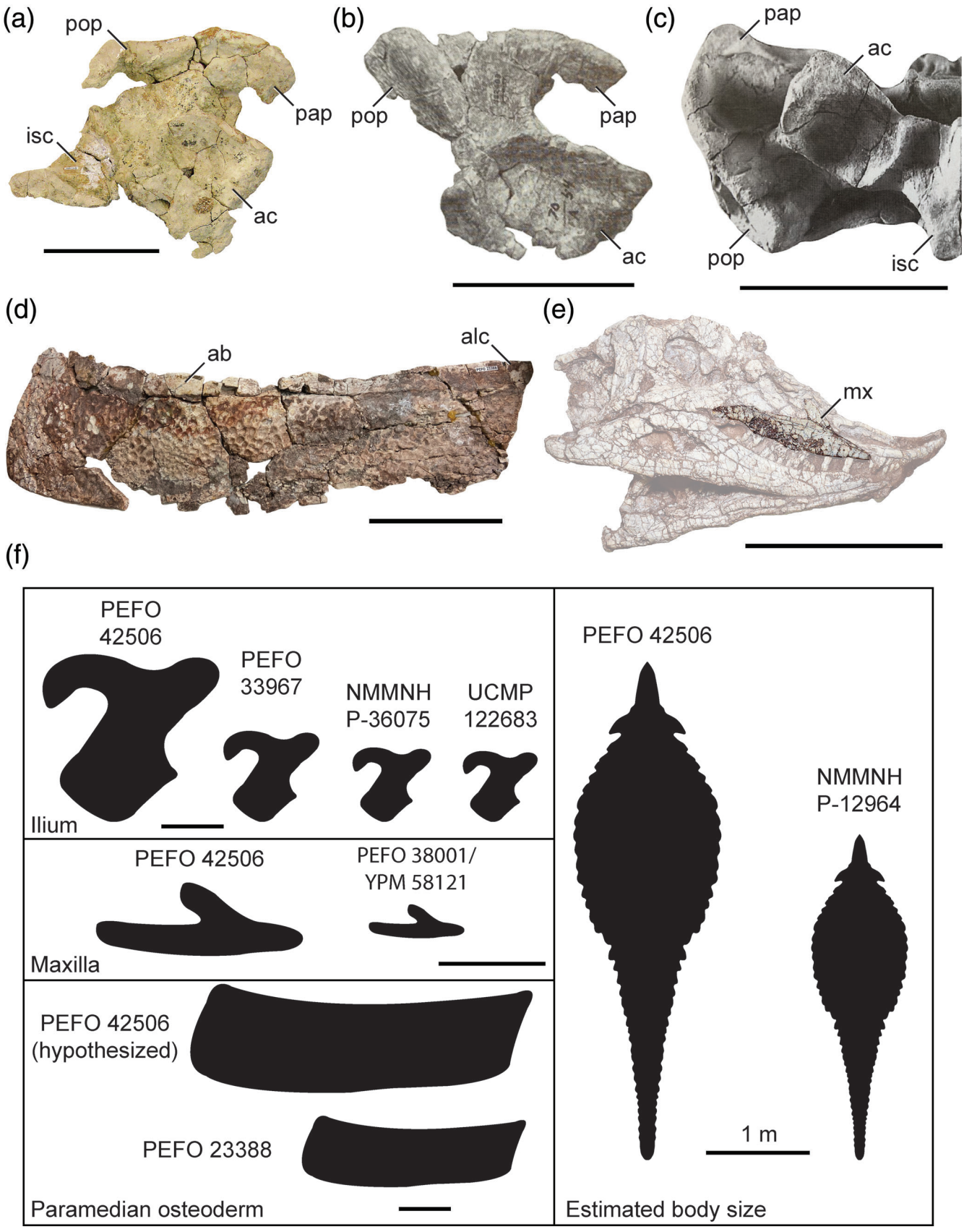

FIGURE 2 Legend on next page.

tetrapods (e.g., mosasaurs, Waskow & Sander, 2014; non-archosaur archosauromorphs, de Ricqlès et al., 2008; theropods, Erickson et al., 2004; sauropods, D'Emic et al., 2015; and pseudosuchians, Scheyer & Sues, 2017). Recently, Waskow and Mateus (2017) histologically sampled the ribs of crocodylomorph and dinosaurian archosaurs to assess ontogenetic signals. The authors found that the proximal end of the rib shaft preserves the best growth record near the posteromedial margin by recording more lines of arrested growth, or LAGs, which is most likely due to the anisometric growth of the ribs (Waskow & Sander, 2014). Thus, the ontogenetic information derived from rib histology may be comparable to that obtained from a limb or osteoderm when those are unavailable (Erickson et al., 2004; Waskow & Mateus, 2017; Waskow & Sander, 2014).

In this study, we assess the body size of PEFO 42506 using various proportional comparisons to other aetosaur taxa, particularly other specimens of *T. coccinarum*. Additionally, we histologically sample a trunk rib of PEFO 42506 with the goal of (1) observing growth indicators of the internal bone structure in a large, if not, hypothetically skeletally mature specimen of *T. coccinarum*; and (2) determining if maximum individual body size is correlated with skeletal maturity in some aetosaurs. Histological images associated with this study are available as Morphobank project P4879.

Institutional abbreviations—DMNH, Perot Museum of Nature and Science, Dallas, Texas, USA; GR, Ghost Ranch, Abiquiu, New Mexico, USA; MNA, Museum of Northern Arizona, Flagstaff, Arizona, USA; NMMNH, New Mexico Museum of Natural History and Science, Albuquerque, New Mexico, USA; NHMUK, Natural History Museum, United Kingdom; PEFO, Petrified Forest National Park, Arizona, USA (PFV refers to a vertebrate locality number from PEFO); PVL, Paleontología de Vertebrados, Instituto "Miguel Lillo," San Miguel de Tucumán, Argentina; SMSN, Staatliches Museum für Naturkunde, Stuttgart, Germany; TTU-P, Museum of Texas Tech, Lubbock, Texas, USA; UCMP, University of California Museum of Paleontology, Berkeley, California, USA; UMMP, University of Michigan Museum of Paleontology, Ann Arbor, Michigan, USA; YPM, Yale Peabody Museum, New Haven, Connecticut, USA; ZPAL, Institute of Paleobiology, Polish Academy of Sciences, Warsaw, Poland.

2 | METHODS AND MATERIALS

2.1 | Collection

The new specimen of *Typothorax* (PEFO 42506) was collected from Petrified Forest National Park vertebrate locality PFV 453 (Puerco Ridge N). The specimen is from the Petrified Forest Member of the Chinle Formation (sensu Martz et al., 2012) and consists of both ilia, the right ischium, the right maxilla, one trunk centrum, at least five trunk neural arches, and at least 11 trunk ribs, mostly from the left side (Figure 1). No osteoderms were recovered with the specimen but, fortunately, the shape of the ilium is diagnostic for *Typothorax* within Aetosauria (Martz, 2002; see below). All elements were found associated and all pertain to a single individual of *Typothorax*.

2.2 | Systematic paleontology

Archosauria Cope, 1869, sensu Gauthier & Padian, 1985
Pseudosuchia Zittel, 1887–1890, sensu Gauthier & Padian, 1985
Aetosauria Marsh, 1884, sensu Parker, 2007
Typothoracinae von Huene, 1915, sensu Parker, 2016
Typothorax coccinarum Cope, 1875
Referred specimen: PEFO 42506
Stratigraphic Horizon and Geologic Age: Petrified Forest Member (Chinle Formation). Late Triassic, middle Norian, Revueltian Land Vertebrate Estimated Holochronozone (Martz and Parker, 2017).
Maturity Assessment: Skeletally immature based on the open neurocentral sutures in the trunk vertebral series (Griffin et al., 2020).

2.3 | Taxonomic assignment

Specimens are traditionally assigned to *T. coccinarum* based on the presence of diagnostic paramedian osteoderms, which are characterized by an ornamentation

FIGURE 2 Elements of comparative specimens of *Typothorax coccinarum*. (a) right ilium (PEFO 33967) in lateral view; (b) right ilium (UCMP 122683; modified from Long & Murry, 1995) in lateral view; (c) right half of articulated pelvic girdle (NMMNH P-36075; modified from Lucas et al., 2002) in ventral view; (d) right trunk paramedian osteoderm (PEFO 23388) in dorsal view; (e) skull (PEFO 38001/YPM 58121; modified from Reyes et al., 2020) in right lateral view; (f) comparative elements represented by scaled silhouettes and estimated body sizes of *Typothorax coccinarum* (dorsal outline modified from Heckert et al., 2010). ab, anterior bar; ac, acetabulum; alc, anterolateral corner; isc, ischium; mx, maxilla; pap, preacetabular process; pop, postacetabular process. Scale bars equal 10 cm except where noted.

pattern consisting of random circular pits (Heckert et al., 2010; Long & Ballew, 1985; Long & Murry, 1995; Martz, 2002). PEFO 42506 comprises no osteoderms; however, the ilium (Figure 1a) of *T. coccinarum* is very distinctive among aetosaurs (Martz, 2002). PEFO 42506 bears an iliac blade with an extremely anteroposteriorly elongate and distinctly ventromedially curved preacetabular process, very similar to that of UCMP 122683, an unambiguous specimen of *T. coccinarum* (Figure 2; Long & Murry, 1995; Martz, 2002). The postacetabular process of the ilium does not project posteriorly far past the posterior end of the ischiadic peduncle. The end of the preacetabular process is blunt, not pointed, and mediolaterally thickened, forming a distinct knob-like end. This differs from the condition found in all other aetosaurs with known pelvic material where the preacetabular process is often reduced and triangular in lateral view (e.g., *Aetosauroides scagliai*; Casamiquela, 1967; Heckert & Lucas, 2002), and the postacetabular process is more anteroposteriorly elongate and not mediolaterally thickened (e.g., *D. spurensis*; Parker, 2008). This allows for referral of the ilia and associated material of PEFO 42506 to *Typothorax*.

The preserved maxilla in PEFO 42506 (Figure 1c) has an elongate anterior process and the margin along the dorsal process and anterior process is gently curved and anteriorly sloping. This is very similar to what is seen in other known skulls of *T. coccinarum* (PEFO 38001/YPM VP.58121, Reyes et al., 2020; NMMNNH P-12964, Heckert et al., 2010) and differs significantly from the shorter, more triangular anterior process of the maxilla seen in other aetosaurs such as *Paratypothorax andressorum* (SMNS 19003, Schoch & Desojo, 2016) and *Aetosaurus ferratus* (SMNS 5770 S-16, Schoch, 2007). The maxillae of *D. smalli* (TTU-P9023, Small, 2002), *Stagonolepis robertsoni* (NHMUK PV R 4787, Walker, 1961), and *Stagonolepis olenkae* (ZPAL AbIII 574, Sulej, 2010) also have elongate anterior processes, but not to the extent present in *Typothorax*. Combined with the ilium, the anatomy of these elements supports the assignment of this material to *Typothorax*.

Typothorax currently includes only a single recognized species, *T. coccinarum*, with other proposed species demonstrated as ontogenetically variable specimens of the same taxon (Parker & Martz, 2011). Therefore, PEFO 42506 is referred to as the species *T. coccinarum*, pending further revision of the genus and closely related taxa.

2.4 | Histological preparation

We histologically sampled one of the larger ribs of PEFO 42506 at two locations, near the proximal and distal third of the shaft (Figure 1d–f) to determine if the same signals are observed on opposite ends. Based on the results of Waskow and Mateus (2017), we hypothesized that the proximal end sample would preserve the most accurate growth record. The proximal and distal cross-sections of the rib were chosen based on the occurrences of natural breaks in the regions of interest along the shaft. The bones of PEFO 42506 are coated by a thick oxidized iron-rich mineral (Figure 1e,f). We decided against mechanically removing this mineral because we did not want to risk losing any data from the sub-periosteal surface. Molds and casts of the rib samples were created using a 1:1 ratio of PlatSil® 73-25 silicon rubber and EasyFlo 60 liquid plastic. The matrix-covered rib samples were individually embedded in resin using 1.5 oz Silmar plus 15 drops of MEKP and air bubbles were removed with a vacuum chamber. As we polished a surface of the resin block, we noticed that the matrix was flaking away which made the mounting onto the glass slide susceptible to air pockets. To mediate this, we stabilized the samples by adding PaleoBOND in a vacuum chamber to fill air bubbles. The resin surface was later repolished, and the samples were mounted onto glass slides using Devcon 2-ton epoxy. Once cured, the samples were cut to a thickness of ~4 mm and then ground to optical clarity using abrasive papers of increasing grit size (120/P120, 400/P800, 600/P1200). Samples were analyzed and photographed using the petrographic microscope Zeiss AXIO Imager.M2m.

2.5 | Body size estimation

Following Martz (2002) the maximum anteroposterior length and the maximum dorsoventral height of the ilium were used to proportionately compare the ilium of PEFO 42506 to that of other well-preserved *Typothorax* specimens (with associated osteoderms) to estimate body size (Figure 2f; Table 1). Additionally, the maxillae of known *Typothorax* specimens (i.e., PEFO 38001/YPM VP.58521, Reyes et al., 2020) were compared in size using the maximum anteroposterior length and dorsoventral height (Table 1). The vertebrae of PEFO 42506 were not used for proportional comparisons because of the uncertainty in their position within the trunk sequence.

3 | RESULTS

3.1 | Body size

Preservation of the ilium and maxilla in PEFO 42506 allows for comparisons with known *Typothorax*

TABLE 1 Measurements (mm) of select elements.

	PEFO 42506	PEFO 33967	YPM VP.58521	UCMP 122683	NMMNH P-36075	
Ilium						
Iliac blade length	280	155	N/A	120	125	
Ilium height	275	150	N/A	110	95	
Acetabulum height	165	75	N/A	55	45	
Acetabulum width	200	90	N/A	97	57	
Acetabulum W/H	1.21	1.2	N/A	1.76	1.27	Ratio
Maxilla						
Length	187	N/A	90	N/A	N/A	
Height	69	N/A	29	N/A	N/A	
Trunk vertebra						
Transverse process width	154	N/A	N/A	N/A	N/A	
Spine table width	6	N/A	N/A	N/A	N/A	
Neural arch height	141	N/A	N/A	N/A	N/A	
Neural spine height	90	N/A	N/A	N/A	N/A	
Osteoderms						
Paramedian A width	N/A	200	N/A	N/A	216	
Paramedian A length	N/A	80	N/A	N/A	84	
Paramedian A W/L	N/A	2.5	N/A	N/A	2.6	Ratio
Paramedian B width	N/A	225	N/A	N/A	210	
Paramedian B length	N/A	70	N/A	N/A	75	
Paramedian B W/L	N/A	3.2	N/A	N/A	2.8	Ratio

specimens to observe size variation across the taxon in the Chinle Formation and Dockum Group (Figure 2). Three well-preserved *Typothorax* ilia are PEFO 33967 (Figure 2a,f) from the Petrified Forest Member (Chinle Formation) of Arizona, UCMP 122683 (Figure 2b,f) from the Petrified Forest Member of New Mexico (Long & Murry, 1995; Martz, 2002), and NMMNH P-36075 (Figure 2c,f) from the Tres Lagunas Member of the Santa Rosa Formation (Lucas et al., 2002). The ilium of PEFO 42506 (Figures 1a and 2f; Table 1) has a maximum anteroposterior length of 28 cm and maximum dorsoventral height of 27.5 cm. UCMP 122683 has a maximum anteroposterior length of 12 cm and maximum dorsoventral height of 11 cm; they equate to 43% and 40% of those respective measurements in PEFO 42506. PEFO 33967 exhibits a maximum anteroposterior length of 15.5 cm and maximum dorsoventral height of 15 cm; they both equate to 55% of those respective measurements in PEFO 42506. NMMNH P-36075 has a maximum anteroposterior length of 12.5 cm and maximum dorsoventral height of 9.5 cm (Table 1); they equate to 45% and 35% of those respective measurements in PEFO 42506. Additionally, the maxilla of PEFO 38001/YPM VP.58521 (Figure 2e,f; Table 1) has a maximum anteroposterior length of 8.5 cm and maximum dorsoventral height of 2.9 cm, which equate to 45% and 42% of those respective measurements (length = 18.7 cm; height = 6.9 cm) of PEFO 42506 (Figure 1c).

3.2 | Histology

3.2.1 | Proximal sample

The thin section (Figure 3a) highlights the thick mineral coat on the bone surface (Figure 1d,f). Cracks and eroded spaces permineralized by calcite are visible in cross-section. The extent of this permineralization varies throughout the bone; the periosteum and compact bone have been partially degraded with cracks running perpendicular and parallel to the surface, resulting in many bone fragments being assimilated within the matrix itself (Figure 3c,e). Permineralization is greatest medially as the rib is mostly eroded/remodeled and replaced by calcite (Figure 3e). Proximally, the rib is predominantly coarse cancellous bone with the medullary region trending in a transverse lateromedial direction. The layer of compact bone is thin, but in general it is thickest

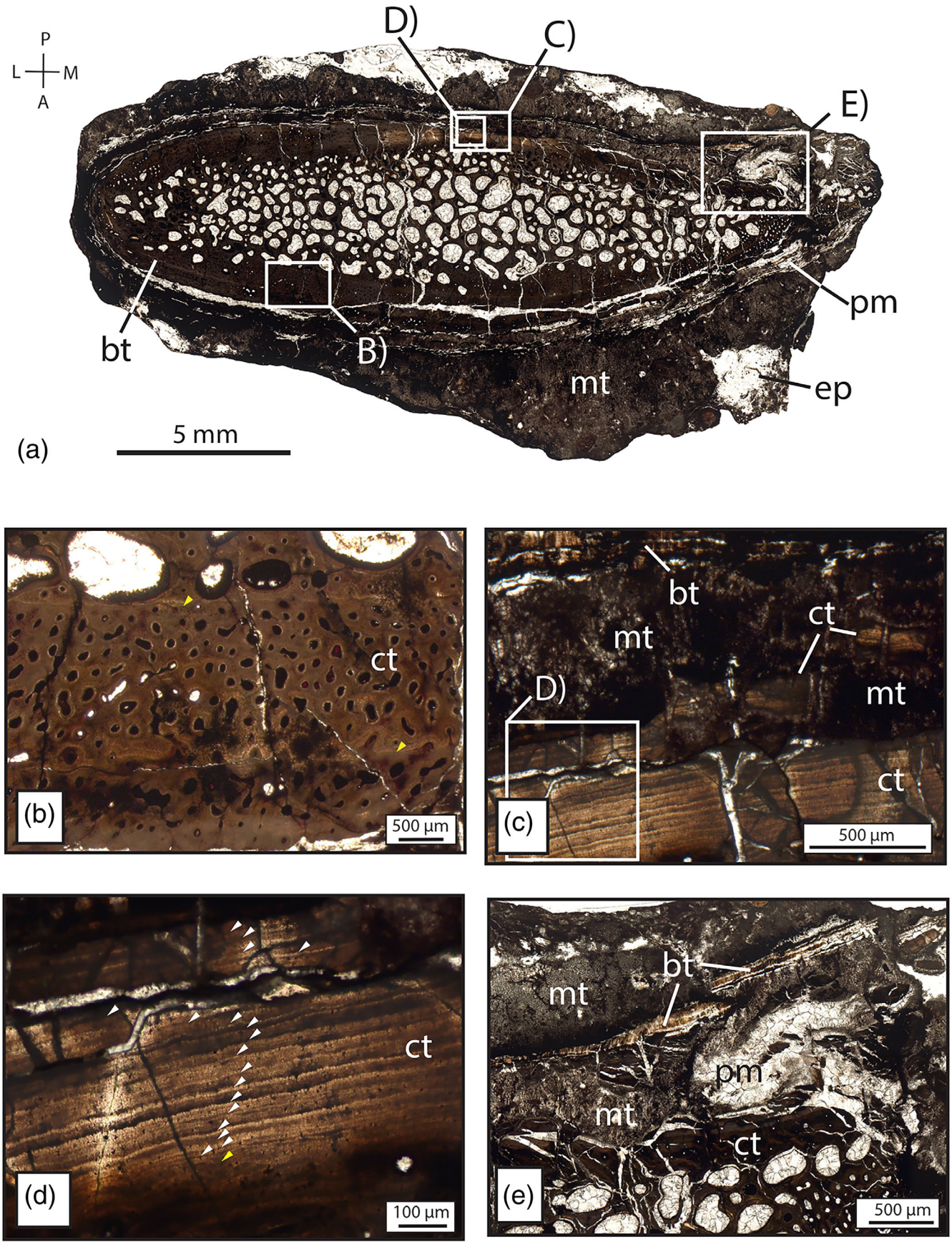

FIGURE 3 Legend on next page.

anteriorly (Figure 3a). Evidence of endosteal resorption of the compact bone is most notable posteromedially. Anteriorly, the compact bone preserves two resorption boundaries (Figure 3b), indicating two different intervals of endosteal bone resorption. The compact bone shows evidence of significant secondary remodeling throughout the rib sample, particularly in the posterior margin.

Anteriorly and posterolaterally, the cortical bone exhibits a vascularized reticular to longitudinal pattern. Posteromedially, there is a section of lamellar fabric tissue in the cortex that is predominantly unremodeled and poorly vascularized (Figure 3c,d). This area shows a decrease in the density of osteocyte lacunae periosteally. This is the only region of compact bone that preserves lines of arrested growth (LAGs; Figure 3c,d), which represent the slowing or complete cessation of growth (de Ricqlès et al., 2021; Francillon-Vieillot et al., 1990; Huttenlocker et al., 2013; Tucker, 1997; Woodward et al., 2011). Although this region of the proximal rib sample preserves the most accurate growth data, the outer rim of the bone has been partially assimilated into the matrix (Figure 3c,e), including some of the outer LAGs. Thus, LAG count suggests a minimum age of around 16–19 years (see discussion). A resorption boundary is evident near the endosteal margin of the compact bone (Figure 3d) suggesting that some LAGs deposited early in life may have been lost due to bone resorption. The spacing between the LAGs decreases periosteally, yet there is no clear evidence of an external fundamental system (EFS), which is deposited in a range of vertebrates (e.g., mammals, non-avian dinosaurs, and some reptiles) as skeletal maturity is reached (Woodward et al., 2011, 2013). It is possible that the region of the cortex that would preserve the EFS has been too degraded by the interface with the matrix, but there is also no evidence of an EFS in the fragments of bone that have been assimilated into the matrix (Figure 3c).

3.2.2 | Distal sample

The distal sample (Figure 4a) of the rib shaft is similar to the proximal sample mentioned above (Figure 3a) in that it is predominantly coarse cancellous bone (Figure 1d,e–g). Most of the compact cortex is preserved, but it is thickest posteriorly, unlike the proximal sample. The outer sub-periosteal surface of the distal sample exhibits a high degree of permineralization (Figure 4b,c,e). Unfortunately, the medial portion of the rib cross-section was ground too thin during slide preparation resulting in the loss of some bone, but it is apparent that this area exhibited extensive secondary remodeling (Figure 4c). The cortex is not as degraded as the proximal sample, but there is a large crack running anteroposteriorly that was diagenetically filled with calcite (Figure 4a,b). The cortex exhibits longitudinal patterning and extensive secondary remodeling. Unlike the proximal sample, there is no evidence of LAGs on the posteromedial region of the distal rib sample (Figure 4b). This is most likely related to the growth trajectory of the rib from the proximal to distal end as noted by Waskow and Sander (2014). Anteriorly, the compact bone preserves two continuous resorption boundaries (Figure 4d), indicating two different intervals of endosteal bone resorption. There appear to be approximately six LAGs present near the resorption boundaries in this region of the cortex, but they are separated by an area of extensive secondary remodeling (Figure 4d).

4 | DISCUSSION

4.1 | Body size estimate

Based on known specimens, *Typothorax* was thought to be a mid-sized aetosaur with a maximum body length of 3–4 m (Desojo et al., 2013; Heckert et al., 2010; Long & Murry, 1995). However, the size discrepancies (Figure 2f) between PEFO 42506 and known specimens of *Typothorax* with overlapping skeletal elements (i.e., PEFO 33967, Figure 2a; UCMP 122683, Figure 2b; NMMNH-P 36075, Figure 2c; PEFO 38001/YPM VP.58521, Figure 2e) are extreme, with PEFO 42506 being nearly twice the size of the largest individual mentioned above (Figure 2f). Unfortunately, no osteoderms were recovered with PEFO 42506, but at that scale the mediolateral width of a dorsal pelvic paramedian osteoderm would be approximately 50 cm based on those found in other *Typothorax* specimens (e.g., PEFO 33967). In *Typothorax*, dorsal pelvic paramedian osteoderms are some of the mediolaterally narrower osteoderms in the carapace, as a trunk paramedian would

FIGURE 3 Histological images of the proximal sample of the trunk rib of PEFO 42506. (a) whole image of proximal histological section with regions of interest bounded by squares; (b) resorption boundaries in the anterior region of the cortex; (c) posteromedial region of the cortex with lines of arrested growth (LAGs) partially intermixed into the matrix; (d) magnified region of the cortex in (c) used to determine LAG count; (e) medial region of the cortex showing extensive remodeling and permineralization. Images of slides are in plane polarized light. White arrows = estimated LAGs; yellow arrows = resorption boundaries. A, anterior; bt, bone tissue; ct, cortex; ep, epoxy; L, lateral; M, medial; mt, matrix; P, posterior; pm, permineralization.

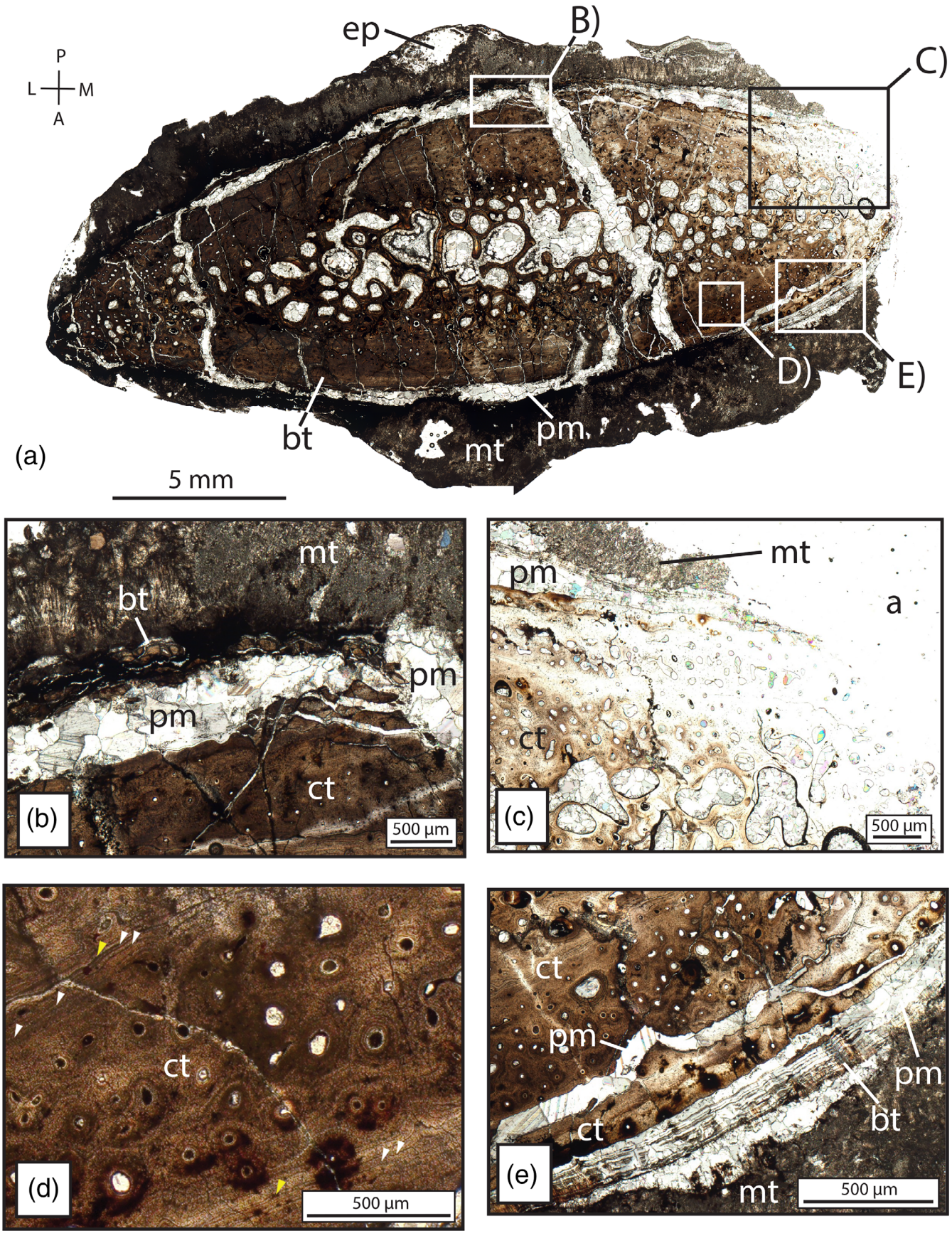

FIGURE 4 Legend on next page.

be another 25%–30% of that width near the center of the trunk (Heckert et al., 2010); this would result in a dorsal trunk paramedian osteoderm in PEFO 42506 with an approximate mediolateral width of 65 cm (Figure 2f). Heckert et al. (2010) estimated a maximum dorsal trunk paramedian osteoderm mediolateral width of 43 cm for a large *T. coccinarum* specimen from the Bull Canyon Formation of New Mexico (NMMNH P-12964). Using size as a proxy, the authors hypothesized that NMMNH P-12964 represents an individual of *Typothorax* that is nearing or at skeletal maturity. Thus, Heckert et al. (2010) argued that NMMNH P-12964 preserved the largest paramedian osteoderms known for *Typothorax* and that this taxon exhibited a maximum body length of 3 m (Figure 2f). Another paramedian osteoderm of *T. coccinarum* (PEFO 23388; Figure 2d,f), also from the Petrified Forest Member at PEFO, has a maximum mediolateral length of 42.6 cm and a maximum anteroposterior width of 11.3 cm, making it slightly smaller than NMMNH P-12964. Considering the large size of the dorsal trunk paramedian osteoderms observed in NMMNH P-12964 and PEFO 23388 (Figure 2d), they are still more than one-third smaller than those we hypothesize would be present in PEFO 42506 based on the size of the ilia (Figure 2f), if those elements grew isometrically.

The ilia of PEFO 42506 (Figures 1a and 2f) are the largest recorded aetosaur ilia yet known. A very large specimen of *D. spurensis* (MNA V9300; Parker, 2008) with an estimated body length >5 m (Parker, 2008) has an approximate ilium dorsoventral height of 20 cm and maximum anteroposterior length of 23.5 cm. These measurements are 71% and 85% of the same measurements in PEFO 42506, respectively. An isolated right ilium (UMMP 7322) from the Dockum Group of Texas that Long and Murry (1995, fig. 92) assigned to *D. spurensis* has a maximum anteroposterior length of 27.5 cm and a dorsoventral height of 18.4 cm, which are 98% and 67%, respectively, the same measurement in PEFO 42506. Thus, proportionally PEFO 42506 is the largest known aetosaur specimen with a body length probably >5 m based on comparison with MNA V9300 (see Parker, 2008). This is supported further by the size of the associated maxilla. The maxilla of PEFO 42506 (Figure 1c) is more than double the anteroposterior length and dorsoventral height of that observed in *Typothorax* specimen PEFO 38001/YPM VP.58521 (Figure 2f). Reyes et al. (2020) hypothesized that PEFO 38001/YPM VP.58521 exhibited a body length of at least 2.1 m based on proportional comparisons to other aetosaur taxa. These measurements further support our proportional analysis indicating that PEFO 42506 represents an individual of *Typothorax* with a body length >5 m.

4.2 | Ontogenetic size indicators

The neural arches (Figure 1b) on the trunk vertebrae of PEFO 42506 have elongate transverse processes with both the diapophysis and parapophysis preserved, and a tall neural spine with an expanded spinal table. In all these vertebrae the neurocentral sutures are not co-ossified (Figure 1b), which is considered an indicator of an individual that has not reached an advanced ontogenetic stage in some pseudosuchians (Brochu, 1996; Irmis, 2007). Considering its large size, this would suggest that PEFO 42506 had not yet reached skeletal maturity, which is remarkable considering its large size. Yet, smaller specimens of *Typothorax* (i.e., AMNH 7634, PEFO 33937, TTUP-9214) that are less than half the size of PEFO 42506, exhibit vertebrae with co-ossified neurocentral sutures (Irmis, 2007; Martz, 2002). Irmis (2007) and Griffin et al. (2020) discuss the disparity in the timing of the closure of the neurocentral sutures making this proxy limited in the absence of independent histological analysis. Griffin et al. (2020) noted that two relatively large individuals of *Coelophysis bauri* exhibit open neurocentral sutures unlike the smaller individuals described by Griffin (2018). PEFO 42506 appears to exhibit a similar condition as seen in *C. bauri*, in which large individuals of these taxa may lack co-ossified neurocentral sutures whereas they can be completely co-ossified in smaller individuals. TTUP-9214 is considered a skeletally immature specimen of *T. coccinarum* based on its approximate body length of 2 m, and the fact that the neural arches are partially co-ossified with their respective centra in the cervical, trunk, and caudal regions (Martz, 2002); the neural arches are attached to the respective centra, unlike PEFO 42506; however, the sutures are clearly discernable indicating that they are not completely co-ossified with each other (Martz, 2002). The degree of

FIGURE 4 Histological images of the distal sample of the trunk rib of PEFO 42506. (a) whole image of distal histological section with regions of interests bounded by squares; (b) posterior region of the cortex showing thick regions of permineralization; (c) medial region of the bone that was grounded too thin during slide preparation; (d) LAGs and resorption boundaries in the anterior region of the cortex. Images of slides are in plane polarized light; (e) anteromedial region of cortex intermixed with permineralization. White arrows = estimated LAGs; yellow arrows = resorption boundaries. A, anterior; a, air; bt, bone tissue; ct, cortex; ep, epoxy; L, lateral; M, medial; mt, matrix; P, posterior; pm, permineralization.

co-ossification in the vertebrae of TTUP-9214 aligns with the observations of the vertebra in *C. bauri* (Griffin et al., 2020). Because of the disparity in the pattern and timing of the sequence, particularly with respect to body size, the use of neurocentral sutures to assess maturity should be limited to specific groups in the absence of independent histological evidence (Irmis, 2007; Griffin et al., 2020). In this case, specimen size and presence of open neurocentral sutures conflicted in the determination of skeletal maturity, thus we decided to hypothesize the skeletal maturity of PEFO 42506 through histological analysis of a trunk rib.

The bone tissue (Figures 3 and 4) of PEFO 42506 indicates that this individual exhibited high bone remodeling and slow growth (Huttenlocker et al., 2013; Woodward et al., 2013; de Buffrénil et al., 2021). The spacing between the LAGs decreases periosteally (Figure 3c,d) indicating that growth was slowing down (Lee et al., 2013). Histological studies on extant crocodylomorphs show that as the specimen reaches skeletal maturity, skeletal growth slows down and LAG spacing decreases radially (Woodward et al., 2011), however Cullen et al. (2021) demonstrate that decreased LAG spacing might be expected regardless of growth rate due to the relationship between circumference and cross-sectional area of the sampled element.

The posteromedial region of the proximal sample (Figure 3d; where the LAGs are preserved) shows no evidence of high vascularity or high levels of disorganization (i.e., woven bone tissue) which are suggestive of fast growth (de Boef & Larsson, 2007; de Buffrénil & Quilhac, 2021; Parker et al., 2021). Previous histological studies (e.g., Cerda et al., 2018; Cerda & Desojo, 2011; de Ricqlès et al., 2021; Hoffman et al., 2019; Paes-Neto et al., 2021; Parker et al., 2008; Ponce et al., 2023; Scheyer et al., 2014; Taborda et al., 2013; Teschner et al., 2022, 2023; Werning, 2013) sampling aetosaur limbs and osteoderms arrived at the same interpretations, suggesting that aetosaurs exhibited growth rates similar to extant crocodylians (de Ricqlès et al., 2003; Parker et al., 2008) or possibly even slower (Taborda et al., 2013). Recent histological studies found that some aetosaurs (i.e., *Coahomasuchus chathamensis*; *Aetosauroides scagliai* = "*Polesinosuchus aurelioi*"; typothoracine juvenile specimen, GR 252) exhibited periods of rapid bone deposition as indicated by the presence of woven-fibered bone tissue (Hoffman et al., 2019; Paes-Neto et al., 2021; Ponce et al., 2023; Werning, 2013), suggesting a disparity in growth rates within the Aetosauria. Cubo et al. (2012) determined that *Typothorax* had low growth rates; however, the specimen they sampled (proximal end of limb bone; UCMP 25905) is from the *Placerias* Quarry (UCMP A269) of Arizona. The stratigraphic position of that site (lower Chinle Formation) and the lack of distinguishing apomorphies in the element almost certainly preclude it from being assignable to *Typothorax*, which does not occur at that site (Long & Murry, 1995; Parker, 2018; Reyes et al., 2023).

This disparity in growth rates among aetosaurs aligns with histological analyses of *A. mississippiensis* (Woodward et al., 2014), where the bone tissue indicates that this taxon exhibits brief periods of fast growth (woven tissue) early in ontogeny but, overall, the growth rate is slow (lamellar to parallel-fibered tissue organization). Woodward et al. (2014) suggested that the woven tissue in *A. mississippiensis* likely coincides with optimal environmental conditions promoting rapid skeletal growth. However, a recent study by Grigg et al. (2021) hypothesized that this period of rapid growth in *A. mississippiensis* is an atavistic property associated to its ancestry, where archosauriforms exhibited tachymetabolic endothermy (whole-body endothermy), contrary to historical interpretations arguing that ectothermy is plesiomorphic among archosaurs. This hypothesis aligns with observations of woven fibered tissue in basal pseudosuchians, including aetosaurs (Hoffman et al., 2019; Paes-Neto et al., 2021; Werning, 2013).

The most complete sequence of LAGs is observed in the posteromedial cortex of the proximal rib sample of PEFO 42506 (Figure 3c,d), a feature documented in proximal rib sections of other archosaur taxa (Waskow & Mateus, 2017; Waskow & Sander, 2014). These LAGs represent the slowing or temporal cessation of skeletal growth (Woodward et al., 2011). Among ectothermic reptiles (e.g., crocodylians), the slowing and/or cessation of skeletal growth can reflect the animal's inability to adjust to seasonal stress (e.g., changes in temperature, precipitation, sunlight exposure), either directly and/or indirectly (e.g., influencing physiology, food resources; Rootes et al., 1991; Köhler et al., 2012; Werning, 2013; Rainwater et al., 2021). Because of the relationship between skeletal growth and seasonal variation, LAGs, or LAG 'packets' (group of associated LAGs) are hypothesized to represent a yearly cessation of growth (Tucker, 1997; Werning, 2013; Woodward et al., 2013). Therefore, because of the relationship between skeletal growth and seasonal variation, LAG or LAG 'packet' counts can be used as a proxy for absolute age (Griffin et al., 2020; Woodward et al., 2013).

Paleosol data of the Petrified Forest Member of the Chinle Formation, the stratigraphic unit from which PEFO 42506 was collected, indicates that the environment was semi-arid with variations in annual precipitation and temperatures, which have been related to the shift in tectonics and northern movement of the North American plate associated with the rifting of Pangea during the Norian (Atchley et al., 2013; Dubiel & Hasiotis, 2011; Nordt et al., 2015). Based on the relationship observed between skeletal growth and environmental

stress among extant crocodylomorphs, we hypothesize that environmental seasonal stress (i.e., yearly flux in precipitation and temperature) influenced the skeletal growth of aetosaurs to some extent. Thus, the LAGs observed in the proximal rib sample of PEFO 42506 (Figure 3c,d) are hypothesized to represent a yearly cessation of growth allowing for an absolute age count.

Previous histological studies on osteoderms of the aetosaurs *Paratypothorax andressorum* (SMNS 91551; Scheyer et al., 2014) and *Aetosauroides scagliai* (PVL 2052; Taborda et al., 2013; Cerda et al., 2018) found that these taxa lived a minimum of 17–22 years, respectively, indicating that some aetosaurs could live beyond two decades. The LAG count on the proximal rib sample suggests that PEFO 42506 lived a minimum of 16–19 years prior to death (Figure 3d). This age is a minimum estimate because: (1) endosteal resorption of the primary tissue in the inner cortex can result in the loss of LAG data, thus eliminating records of early growth (Parker et al., 2008; Tucker, 1997; Woodward et al., 2011); (2) the incorporation of the outer bone cortex into the matrix seen in the proximal sample (Figure 3c,e) may have resulted in the loss of LAG data; (3) there can be variation in LAG count between ribs and limb elements (Cullen et al., 2020; Heck & Woodward, 2021; Waskow & Sander, 2014; Woodward et al., 2014); and (4) age studies on wild crocodylians (e.g., *Crocodylus johnstoni*) with known ages (up to 20 years) indicate that there is a ± 1-year age variation between the known age of an individual and age based on LAG count within a post-occipital osteoderm (Tucker, 1997). Thus, it is evident that age estimates based on osteoderm histology can be offset from the actual age (Tucker, 1997), and is likely associated with the delay in the timing of ossification between osteoderms and the endoskeleton (Vickaryous & Hall, 2008).

The LAG data observed in PEFO 42506 aligns with these previous observations, despite PEFO 42506 being a much larger individual. In the compact bone of the proximal part of the rib (Figure 3c,d), the LAGs become more tightly spaced periostealy, yet there is no clear evidence of an EFS. Previous studies (e.g., Cullen et al., 2020, 2021; Padian et al., 2016) determined that there can be variation in the development of an EFS between bones that experience different mechanical stresses (e.g., rib versus femur). It is evident that elements freed of weight-bearing stress (e.g., gastralia, ribs) will develop an EFS sooner than a weight-bearing limb element (e.g., femur) to grow allometrically within the same individual (Cullen et al., 2020; Padian et al., 2016). Thus, the presence of an EFS in a rib does not imply that asymptotic growth had yet been achieved in the femur or that an EFS would be present within this element. Although PEFO 42506 does not preserve any limb elements, the absence of an EFS within the sampled trunk rib (Figure 3d) does imply that an EFS is absent within the femur of this individual. Based on our data and current understanding of the discordance in the development of an EFS between skeletal elements (Cullen et al., 2020; Padian et al., 2016), we infer that PEFO 42506 did not reach skeletal maturity before its death and may have continued growing had it lived longer.

Although we are not able to unambiguously confirm the presence of an EFS in PEFO 42506 (Figure 3c,d), previous studies have documented the presence of an EFS in other aetosaur taxa. For example, Woodward et al. (2011) indicated an EFS within a partial humerus of *Desmatosuchus* sp. (UCMP 3218); but note that (1) the specimen UCMP 3218 is mislabeled in Woodward et al. (2011) and the correct specimen number is UCMP 32178 (de Ricqlès et al., 2003, plate 2.1; Werning, 2013, pg. 63); (2) there are at least four different aetosaur taxa (i.e., *Calyptosuchus wellesi*, *D. smalli*, *D. spurensis*, *Kryphioparma caerula*) present in the *Placerias* Quarry (Long & Murry, 1995; Parker, 2005, 2018; von Baczko et al., 2021; Reyes et al., 2023), so it is possible that UCMP 32178 could possibly belong to *C. wellesi* or *K. caerula* since their humeral anatomy is currently unknown (Parker, 2018; Reyes et al., 2023), and it differs significantly from known humeri of *T. coccinarum* (e.g., TTU-P9124, NMMNH P-12964) and paratypothoracins (e.g., DMNH 9942). Thus, the partial humerus UCMP 32178 should be conservatively assigned to the broader aetosaurian clade Stagonolepidoidea (sensu Parker, 2018). Nonetheless, assuming that UCMP 32178 belongs to *Desmatosuchus* sp., following de Ricqlès et al. (2003) and Woodward et al. (2011), it only represents the proximal portion of a right humerus impeding our ability to estimate the body length of this individual and properly compare it to the data presented here for PEFO 42506. Like *T. coccinarum* (based on PEFO 42506), *D. spurensis* could also exhibit a skeletal length of >5 m as estimated for MNA V9300 (Parker, 2008). It should be noted that the *P. andressorum* (SMNS 91551, paramedian osteoderm fragment) sampled by Scheyer et al. (2014, fig. 7g) appears to exhibit an EFS (based on the tightly packed LAGs near the periosteal margin) although this feature is not described by those authors.

The histological data presented by Woodward et al. (2011) and Scheyer et al. (2014) suggested that aetosaurs did not exhibit indeterminate growth (continued but reduced skeletal growth after sexual maturity is reached; Rainwater et al., 2021). Historically, it has been argued that extant crocodylomorphs exhibit indeterminate growth (Chabreck & Joanen, 1979) but recent long-term studies on both wild and captive populations of *A. mississippiensis*, *C. johnstoni*, and *Caiman yacare* argue that these archosaurs exhibit determinate growth as indicated by their asymptotic body lengths and the presence

of an EFS (Campos et al., 2014; Rainwater et al., 2021; Wilkinson et al., 2016; Woodward et al., 2011). Studies on both extinct and extant archosaurs suggest that determinate growth might be plesiomorphic to Archosauria (Woodward et al., 2011; see extended data, Nesbitt et al., 2017). Thus, it is hypothesized that early-diverging pseudosuchian groups, such as aetosaurs (Desojo et al., 2013), exhibited a maximum body size. PEFO 42506 indicates that some aetosaurs (e.g., desmatosuchins, typothoracines) could exhibit very large body sizes >5 m and possibly maintained indeterminate growth.

5 | CONCLUSIONS

The discovery and osteohistological analysis of PEFO 42506 highlights the size potential and growth of a typothoracine aetosaur. Currently, this specimen represents the largest known specimen of this group and is the largest aetosaur specimen reported, which demonstrates the potential upper size range for the Aetosauria. The non-co-ossified neural central sutures may suggest that this specimen had not yet reached skeletal maturity and the lack of indicators of growth cessation suggests that even larger individuals may have existed. Various specimens of *T. coccinarum* of differing sizes and degrees of neurocentral co-ossification (including PEFO 42506) highlight the discordance in the timing of co-ossification of the neurocentral sutures indicating that no single factor should be used as a reliable proxy for ontogenetic maturity in archosaurs. Thus, a combination of several proxies, including histological analysis, should be used to assess the skeletal maturity of an individual. In this case, histological analysis of a trunk rib shows that PEFO 42506 did not deposit an external fundamental system after as few as 16 years, indicating that it had not reached skeletal maturity before death despite its extremely large body size, and that it may have reached a larger body size >5 m. Finally, the agreement of histological data and neurocentral suture co-ossification indicates that PEFO 42506 was skeletally immature and demonstrates that size is the incongruent indicator and should not be used alone to determine the maturity of an individual (Brochu, 1996; Griffin et al., 2020).

AUTHOR CONTRIBUTIONS

William G. Parker: Conceptualization; investigation; funding acquisition; writing – original draft; methodology; validation; writing – review and editing; project administration; supervision. **William A. Reyes:** Methodology; visualization; writing – review and editing; formal analysis; software; data curation; resources. **Adam D. Marsh:** Methodology; visualization; writing – review and editing; data curation; resources.

ACKNOWLEDGMENTS

We thank Chuck Beightol, Emily Lessner, Ben Kligman, Bryan Gee, and Alexander Beyl for fieldwork. Cathy Lash, Larkin McCormack, Cassi Knight, Nicole Dzenowski, and Tim Allen prepared the specimen. Matt Smith, Pat Holroyd, and Axel Hungerbühler provided access to specimens. Deborah Wagner and Diana Boudreau assisted with the molding, casting, and histological preparation. Rowan Martindale provided training and access to the petrographic microscope used to analyze and photograph the histological sections. Reviews by Chris Griffin and Jeffrey Martz improved the manuscript. This work was supported by the National Science Foundation Graduate Research Fellowship Program under Grant No. 2137420 to William A. Reyes. Any opinions, findings, and conclusions or recommendations expressed in this material are those of the authors and do not necessarily reflect the views of the National Science Foundation or of the United States Government. This is Petrified Forest National Park paleontological contribution no. 88.

ORCID

William G. Parker https://orcid.org/0000-0002-6005-7098
William A. Reyes https://orcid.org/0000-0002-9967-2557
Adam D. Marsh https://orcid.org/0000-0002-3223-8940

REFERENCES

Atchley, S. C., Nordt, L. C., Dworkin, S. I., Ramezani, J., Parker, W. G., Ash, S. R., & Bowring, S. A. (2013). A linkage among pangean tectonism, cyclic alluvation, climate change, and biological turnover in the Late Triassic: The record from the Chinle Formation, southwestern United States. *Journal of Sedimentary Research*, *83*, 1147–1161.

Baczko, M. B. V., Desojo, J. B., Gower, D. J., Ridgely, R., Bona, P., & Witmer, L. M. (2021). New digital braincase endocasts of two species of *Desmatosuchus* and neurocranial diversity within Aetosauria (Archosauria: Pseudosuchia). *The Anatomical Record*, *305*, 2415–2434. https://doi.org/10.1002/ar.24798

Boef, M. D., & Larsson, H. C. E. (2007). Bone microstructure: Quantifying bone vascular orientation. *Canadian Journal of Zoology*, *85*, 63–70.

Brochu, C. A. (1996). Closure of neurocentral sutures during crocodilian ontogeny: Implications for maturity assessment in fossil archosaurs. *Journal of Vertebrate Paleontology*, *16*, 49–62.

Buffrénil, V. D., & Quilhac, A. (2021). Bone tissue types: A brief account of currently used categories. In V. de Buffrénil, A. J. d. Ricqlès, L. Zylberberg, & K. Padian (Eds.), *Vertebrate skeletal histology and paleohistology* (pp. 147–182). CRC Press.

Buffrénil, V. D., Quilhac, A., & Castanet, J. (2021). Cyclical growth and skeletochronology. In V. D. Buffrénil, A. J. D. Ricqlès, L. Zylberberg, & K. Padian (Eds.), *Vertebrate skeletal histology and paleohistology* (pp. 626–640). CRC Press.

Campos, Z., Maurão, G., Coutinho, M., & Magnusson, W. E. (2014). Growth of *Caiman crocodilus yacare* in the Brazilian Pantanal. *PLoS One*, *9*, e89363. https://doi.org/10.1371/journal.pone.0089363

Casamiquela, R. M. (1967). Materiales adicionales y reinterpretacion de *Aetosauroides scagliai*. *Paléo*, *33*, 173–196.

Cerda, I. A., & Desojo, J. B. (2011). Dermal armour histology of aetosaurs (Archosauria: Pseudosuchia), from the Upper Triassic of Argentina and Brazil. *Lethaia*, *44*, 417–428.

Cerda, I. A., Desojo, J. B., & Scheyer, T. M. (2018). Novel data on aetosaur (Archosauria, Pseudosuchia) osteoderm microanatomy and histology: Paleobiological implications. *Palaeontology*, *61*, 721–745.

Chabreck, R. H., & Joanen, T. (1979). Growth rates of American alligators in Louisiana. *Herpetologica*, *35*, 51–57.

Cope, E. D. (1869). Synopsis of the extinct Batrachia, Reptilia, and Aves of North America. *Transactions of the American Philisophical Society*, *14*, 1–252.

Cope, E. D. (1875). Report on the geology of that part of northwestern New Mexico examined during the field-season of 1874; pp. 61–97 of separate issue, 981–1017 of full report in Annual Report upon the Geographical Explorations West of the 100th Meridian [Wheeler Survey], Appendix LL. Annual Report Chief of Engineers for 1875.

Cubo, J., Le Roy, N., Martinez-Maza, C., & Montes, L. (2012). Paleohistological estimation of bone growth rate in extinct archosaurs. *Paleobiology*, *38*, 335–349.

Cullen, T. M., Brown, C. M., Chiba, K., Brink, K. S., Makovicky, P. J., & Evans, D. C. (2021). Growth variability, dimensional scaling, and the interpretation of osteohistological growth data. *Biology Letters*, *17*, 20210383. https://doi.org/10.1098/rsbl.2021.0383

Cullen, T. M., Canale, J. I., Apesteguía, S., Smith, N. D., Hu, D., & Makovicky, P. J. (2020). Osteohistological analyses reveal diverse strategies of theropod dinosaur body-size evolution. *Proceeding of the Royal Society B*, *287*, 20202258. https://doi.org/10.1016/j.crpv.2015.03.002

de Ricqlès, A. J., Buffrénil, V. D., & Laurin, M. (2021). Archosauromorpha: From early diapsids to archosaurs. In V. D. Buffrénil, A. J. d. Ricqlès, L. Zylberberg, & K. Padian (Eds.), *Vertebrate skeletal histology and paleohistology* (pp. 467–485). CRC Press.

de Ricqlès, A. J., Padian, K., & Horner, J. R. (2003). On the bone histology of some Triassic pseudosuchian archosaurs and related taxa. *Annales de Paléontologie*, *89*, 67–101.

de Ricqlès, A. J., Padian, K., Knoll, F., & Horner, J. R. (2008). On the origin of high growth rates in archosaurs and their ancient relatives: Complementary histological studies on Triassic archosauriforms and the problem of a "phylogenetic signal" in bone histology. *Annales de Paléontologie*, *94*, 57–76.

D'Emic, M. D., Smith, K. M., & Ansley, Z. T. (2015). Unusual histology and morphology of the ribs of mosasaurs (Squamata). *Palaeontology*, *58*, 511–520.

Desojo, J. B., Heckert, A. B., Martz, J. W., Parker, W. G., Schoch, R. R., Small, B. J., & Sulej, T. (2013). Aetosauria: A clade of armoured pseudosuchians from the Upper Triassic continental beds. *Geological Society of London Special Publications*, *379*, 203–239.

Dubiel, R. F., & Hasiotis, S. T. (2011). Deposystems, paleosols, and climatic variability in a continental system: The Upper Triassic Chinle Formation, Colorado Plateau, U.S.A. *Society for Sedimentary Geology Special Publication*, *97*, 347–370.

Erickson, G. M., Makovicky, P. J., Currie, P. J., Norell, M. A., Yerby, S. A., & Brochu, C. A. (2004). Gigantism and comparative life-history parameters of tyrannosaurid dinosaurs. *Nature*, *430*, 772–775.

Francillon-Vieillot, H., de Buffrénil, V., Castanet, J., Géraudie, J., Meunier, F. J., Sire, J. Y., Zylberberg, L., & de Ricqlés, A. (1990). Microstructure and mineralization of vertebrate skeletal tissues. In J. G. Carter (Ed.), *Skeletal biomineralization: Patterns, processes and evolutionary trends* (pp. 471–530). Van Nostrand Reinhold.

Gauthier, J., & Padian, K. (1985). Phylogenetic, functional, and aerodynamic analyses of the origin of birds and their flight. In M. K. Hecht, J. H. Ostrom, G. Viohl, & P. Wellnhofer (Eds.), *The beginning of birds: Proceedings of the international archaeopteryx conference* (pp. 185–197). Freunde des Jura Museums.

Griffin, C. T. (2018). Developmental patterns and variation among early theropods. *Journal of Anatomy*, *232*, 604–640.

Griffin, C. T., Stocker, M. R., Colleary, C., Stefanic, C. M., Lessner, E. J., Riegler, M., Formoso, K., Koeller, K., & Nesbitt, S. J. (2020). Assessing ontogenetic maturity in extinct saurian reptiles. *Biological Reviews.*, *96*, 470–525. https://doi.org/10.1111/brv.12666

Grigg, G., Nowack, J., Wilken Bicudo, J. E. P., Bal, N. C., Woodward, H. N., & Seymour, R. S. (2021). Whole body endothermy: Ancient, homologous and widespread among the ancestors of mammals, birds, and crocodylians. *Biological Reviews.*, *97*, 766–801. https://doi.org/10.1111/brv.12822

Heck, C. T., & Woodward, H. N. (2021). Intraskeletal bone growth patterns in the North Island brown kiwi (*Apteryx mantelli*): Growth mark discrepancy and implications in extinct taxa. *Journal of Anatomy*, *239*, 1075–1095.

Heckert, A. B., & Lucas, S. G. (2000). Taxonomy, phylogeny, biostratigraphy, biochronology, paleobiogeography, and evolution of the Late Triassic Aetosauria (Archosauria: Crurotarsi). *Zentralblatt für Geologie und Paläontologie, Teil I, Heft*, *11–12*, 1539–1587.

Heckert, A. B., & Lucas, S. G. (2002). South American occurrences of the Adamanian (Late Triassic: Latest Carnian) index taxon *Stagonolepis* (Archosauria: Aetosauria) and their biochronological significance. *Journal of Paleontology*, *76*, 852–863.

Heckert, A. B., Lucas, S. G., Rinehart, L. F., Celeskey, M. D., Spielmann, J. A., & Hunt, A. P. (2010). Articulated skeletons of the aetosaur *Typothorax coccinarum* Cope (Archosauria: Stagonolepididae) from the Upper Triassic Bull Canyon Formation (Revueltian: early-mid Norian), eastern New Mexico, USA. *Journal of Vertebrate Paleontology*, *30*, 619–642.

Hoffman, D. K., Heckert, A. B., & Zanno, L. E. (2019). Disparate growth strategies within Aetosauria: Novel histologic data from the aetosaur *Coahomasuchus chathamensis*. *The Anatomical Record*, *302*, 1504–1515.

Huene, F. V. (1915). On reptiles of the New Mexico Triassic in the Cope collection. *Bulletin of the American Museum of Natural History*, *34*, 485–507.

Huttenlocker, A. K., Woodward, H. N., & Hall, B. K. (2013). The biology of bone. In K. Padian & E. T. Lamm (Eds.), *Bone histology of fossil tetrapods: Advancing methods, analysis, and interpretations* (pp. 13–34). University of California Press, Berkeley.

Irmis, R. B. (2007). Axial skeleton ontogeny in the Parasuchia (Archosauria: Pseudosuchia) and its implications for ontogenetic determination in archosaurs. *Journal of Vertebrate Paleontology*, *27*, 350–361.

Köhler, M., Marín-Moratalla, N., Jordana, X., & Aanes, R. (2012). Seasonal bone growth and physiology in endotherms shed light on dinosaur physiology. *Nature*, *487*, 358–361.

Lee, A. H., Huttenlocker, A. K., Padian, K., & Woodward, H. N. (2013). Analysis of growth rates. In K. Padian & E. T. Lamm (Eds.), *Bone histology of fossil tetrapods: Advancing methods, analysis, and interpretations* (pp. 217–252). University of California Press, Berkeley.

Long, R. A., & Ballew, K. L. (1985). Aetosaur dermal armor from the Late Triassic of southwestern North America, with special reference to material from the Chinle Formation of Petrified Forest National Park. *Museum of Northern Arizona Bulletin*, *47*, 45–68.

Long, R. A., & Murry, P. A. (1995). Late Triassic (Carnian and Norian) tetrapods from the southwestern United States. *New Mexico Museum of Natural History and Science Bulletin*, *4*, 1–254.

Lucas, S. G., Heckert, A. B., & Hunt, A. P. (2002). A new species of the aetosaur *Typothorax* (Archosauria: Stagonolepididae) from the Upper Triassic of east-central New Mexico. In A. B. Heckert & S. G. Lucas (Eds.), *Upper Triassic stratigraphy and paleontology* (pp. 221–233). New Mexico Museum of Natural History and Science Bulletin 21.

Lucas, S. G., & Hunt, A. P. (1993). Tetrapod biochronology of the Chinle Group (Upper Triassic), western United States. *New Mexico Museum of Natural History and Science Bulletin*, *3*, 327–329.

Marsh, A. D., Smith, M. E., Parker, W. G., Irmis, R. B., & Kligman, B. T. (2020). Skeletal anatomy of *Acaenasuchus geoffreyi* Long and Murry, 1995 (Archosauria: Pseudosuchia) and its implications for the origin of the aetosaurian carapace. *Journal of Vertebrate Paleontology*, *40*, 4. https://doi.org/10.1080/02724634.2020.1794885

Marsh, O. C. (1884). The classification and affinities of dinosaurian reptiles. *Nature*, *31*, 68–69.

Martz, J. W. (2002). The morphology and ontogeny of *Typothorax coccinarum* (Archosauria, Stagonolepididae) from the Upper Triassic of the American Southwest. Master Thesis, Texas Tech University, Lubbock, TX, pp. 279.

Martz, J. W., Parker, W. G., Skinner, L., Raucci, J. J., Umhoefer, P., & Blakey, R. C. (2012). *Geologic map of Petrified Forest National Park. 1:50,000*. Arizona Geological Survey.

Martz, J. W., & Parker, W. G. (2017). Revised formulation of the Late Triassic Land Vertebrate "Faunachrons" of western North America: recommendations for codifying nascent systems of vertebrate biochronology. In K. Ziegler & W. G. Parker (Eds.), *Terrestrial Depositional Systems: Deciphering Complexities Through Multiple Stratigraphic Methods* (pp. 39–125). Elsevier.

Nesbitt, S. J., Butler, R. J., Ezcurra, M. D., Barrett, P. M., Stocker, M. R., Angielczyk, K. D., Smith, R. M. H., Sidor, C. A., Niedźwiedzki, G., Sennikov, A. G., & Charig, A. J. (2017). The earliest bird-line archosaurs and the assembly of the dinosaur body plan. *Nature*, *544*, 484–487.

Nordt, L., Atchley, S., & Dworkin, S. (2015). Collapse of the Late Triassic megamonsoon in western equatorial Pangea, present-day American southwest. *GSA Bulletin*, *127*, 1798–1815.

Padian, K., Werning, S., & Horner, J. R. (2016). A hypothesis of differential secondary bone formation in dinosaurs. *Comptes Rendus Palevol*, *15*, 40–48.

Paes-Neto, V. D., Desojo, J. B., Biacchi Brust, A. C., Schultz, C. L., Da-Rosa, A. A. S., & Soares, M. B. (2021). Intraspecific variation in the axial skeleton of *Aetosauroides scagliai* (Archosauria: Aetosauria) and its implications for the aetosaur diversity of the Late Triassic of Brazil. *Annals of the Brazilian Academy of Sciences*, *93* (Suppl 2), e20201239. https://doi.org/10.1590/0001-3765202120201239

Parker, W. G. (2005). Faunal review of the Upper Triassic Chinle Formation of Arizona. *Mesa Southwest Museum Bulletin*, *11*, 35–54.

Parker, W. G. (2007). Reassessment of the aetosaur '*Desmatosuchus*' *chamaensis* with a reanalysis of the phylogeny of the Aetosauria (Archosauria: Pseudosuchia). *Journal of Systematic Paleontology*, *5*, 41–68.

Parker, W. G. (2008). Description of new material of the aetosaur *Desmatosuchus spurensis* (Archosauria: Suchia) from the Chinle Formation of Arizona and a revision of the genus *Desmatosuchus*. *PaleoBios*, *28*, 1–40.

Parker, W. G. (2016). Revised phylogenetic analysis of the Aetosauria (Archosauria: Pseudosuchia); Assesing the effects of incongruent morphological character sets. *PeerJ*, *4*, e1583. https://doi.org/10.7717/peerj.1583

Parker, W. G. (2018). Redescription of *Calyptosuchus* (*Stagonolepis*) *wellesi* (Archosauria: Pseudosuchia: Aetosauria) from the Late Triassic of the southwestern United States with a discussion of genera in vertebrate paleontology. *PeerJ*, *6*, e4291. https://doi.org/10.7717/peerj.4291

Parker, W. G., & Martz, J. W. (2011). The Late Triassic (Norian) Adamanian–Revueltian tetrapod faunal transition in the Chinle Formation of Petrified Forest National Park, Arizona. *Earth and Environmental Science Transactions of the Royal Society of Edinburgh*, *101*, 231–260.

Parker, W. G., Nesbitt, S. J., Irmis, R. B., Martz, J. W., Marsh, A. D., Brown, M. A., Stocker, M. R., & Werning, S. (2021). Osteology and relationships of *Revueltosaurus callenderi* (Archosauria: Suchia) from the Upper Triassic (Norian) Chinle Formation of Petrified Forest National Park, Arizona, United States. *Journal of Anatomy (early view)*, *305*, 2353–2414. https://doi.org/10.1002/ar.24757

Parker, W. G., Stocker, M. R., & Irmis, R. B. (2008). A new desmatosuchine aetosaur (Archosauria: Suchia) from the Upper Triassic Tecovas Formation (Dockum Group) of Texas. *Journal of Vertebrate Paleontology*, *28*, 692–701.

Ponce, D. A., Desojo, J. B., & Cerda, I. A. (2023). Palaeobiological inferences of the aetosaur *Aetosauroides scagliai* (Archosauria: Pseudosuchia) based on microstructural analyses of its appendicular bones. *Historical Biology*, *35*, 303–314.

Rainwater, T. R., Woodward, H. N., Woodward, A. R., & Wilkinson, P. M. (2021). Evidence of determinate growth in an American alligator (*Alligator mississippiensis*) based on long-term recapture and osteohistological confirmation. *The Anatomical Record (Early View).*, *305*, 3101–3108. https://doi.org/10.1002/ar.24688

Reyes, W. R., Parker, W. G., & Heckert, A. B. (2023). A new aetosaur (Archosauria: Pseudosuchia) from the upper Blue Mesa Member (Adamanian: Early-mid Norian) of the Late Triassic Chinle Formation, northern Arizona, USA, and a review of the

paratypothoracin *Tecovasuschus* across the southwestern USA. *PaleoBios*, *40*, 1–15.

Reyes, W. R., Parker, W. G., & Marsh, A. D. (2020). Cranial anatomy and dentition of the aetosaur *Typothorax coccinarum* (Archosauria: Pseudosuchia) from the Upper Triassic (Revueltian–mid Norian) Chinle Formation of Arizona. *Journal of Vertebrate Paleontology*, *40*, 6. https://doi.org/10.1080/02724634.2020.1876080

Rootes, W. T., Chabreck, R. H., Wright, V. L., Brown, B. W., & Hess, T. J. (1991). Growth rates of American alligators in estuarine and palustrine wetlands in Louisiana. *Estuaries*, *14*, 489–494.

Scheyer, T. M., Desojo, J. B., & Cerda, I. A. (2014). Bone histology of phytosaur, aetosaur, and other archosauriform osteoderms (Eureptilia, Archosauromorpha). *The Anatomical Record*, *297*, 240–260.

Scheyer, T. M., & Sues, H.-D. (2017). Expanded dorsal ribs in the Late Triassic pseudosuchian reptile *Euscolosuchus olseni*. *Journal of Vertebrate Paleontology*, *37*, 1. https://doi.org/10.1080/02724634.2017.1248768

Schoch, R. R. (2007). Osteology of the small archosaur *Aetosaurus* from the Upper Triassic of Germany. *Neues Jahrbuch für Geologie und Paläontologie Abhandlugen*, *246*, 1–35.

Schoch, R. R., & Desojo, J. B. (2016). Cranial anatomy of the aetosaur *Paratypothorax andressorum*. *Neues Jahrbuch für Geologie und Paläontologie Abhandlugen*, *279*, 73–95.

Small, B. (2002). Cranial anatomy of *Desmatosuchus haplocerus* (Reptilia: Archosauria: Stagonolepididae). *Zoological Journal of the Linnean Society*, *136*, 97–111.

Sulej, T. (2010). The skull of an early Late Triassic aetosaur and the evolution of the stagonolepidid archosaurian reptiles. *Zoological Journal of the Linnean Society*, *158*, 860–881.

Taborda, J. R. A., Cerda, I. A., & Desojo, J. B. (2013). Growth curve of *Aetosauroides scagliai* Casamiquela 1960 (Pseudosuchia: Aetosauria) inferred from osteoderm histology. *Geological Society of London Special Publications*, *379*, 413–424.

Teschner, E. M., Konietzko-Meir, D., Desojo, J. B., Schoch, R. R., & Klein, N. (2023). Triassic nursery? Evidence of gregarious behavior in juvenile pseudosuchian archosaurs as inferred by humeral histology of *Aetosaurus ferratus* (Norian; southern Germany). *Journal of Vertebrate Paleontology*, *42*, e2168196.

Teschner, E. M., Konietzko-Meir, D., & Klein, N. (2022). Growth and limb bone histology of aetosaurs and phytosaurs from the Late Triassic Krasiejów locality (SW Poland) reveals strong environmental influence on growth pattern. *Contributions to Zoology*, *91*, 199–232.

Tucker, A. D. (1997). Validation of skeletochronology to determine age of freshwater crocodiles (*Crocodylus johnstoni*). *Marine and Freshwater Research*, *48*, 343–351.

Vickaryous, M. K., & Hall, B. K. (2008). Development of the dermal skeleton in *Alligator mississippiensis* (Archosauria, Crocodylia) with comments on the homology of osteoderms. *Journal of Morphology*, *269*, 398–422.

Walker, A. D. (1961). Triassic reptiles from the Elgin area: *Stagonolepis*, *Dasygnathus* and their allies. *Philosophical Transactions of the Royal Society of London, Series B, Biological Sciences*, *244*, 103–204.

Waskow, K., & Mateus, O. (2017). Dorsal rib histology of dinosaurs and a crocodylomorph from western Portugal: Skeletochronological implications on age determination and life history traits. *Comptes Rendus Pelevol*, *16*, 425–439.

Waskow, K., & Sander, M. P. (2014). Growth record and histological variation in the dorsal ribs of Camarasaurus sp. (Sauropoda). *Journal of Vertebrate Paleontology*, *34*, 852–869.

Werning, S. (2013). Evolution of bone histological characters in amniotes, and the implications for the growth and metabolism. Doctoral Dissertation, University of California, Berkeley, CA, pp. 445.

Wilkinson, P. M., Rainwater, T. R., Woodward, A. R., Leone, E. H., & Carter, C. (2016). Determinate growth and reproductive lifespan in the American alligator (*Alligator mississippiensis*): Evidence from long-term recaptures. *Copeia*, *104*, 843–852.

Woodward, H. N., Horner, J. R., & Farlow, J. O. (2011). Osteological evidence for determinate growth in the American alligator. *Journal of Herpetology*, *45*, 339–342.

Woodward, H. N., Horner, J. R., & Farlow, J. O. (2014). Quantification of intraskeletal histovariability in *Alligator mississippiensis* and implications for vertebrate osteohistology. *PeerJ*, *2*, e422. https://doi.org/10.7717/peerj.422

Woodward, H. N., Padian, K., & Lee, A. H. (2013). Skeletochronology. In K. Padian & E. T. Lamm (Eds.), *Bone histology of fossil tetrapods: Advancing methods, analysis, and interpretations* (pp. 195–215). University of California Press.

Zittel, K. A. (1887–1890). Handbuch der Palaeontologie. 1. Abteilung: Palaeozoologie. 3. Oldenbourg, München & Leipzig.

How to cite this article: Parker, W. G., Reyes, W. A., & Marsh, A. D. (2023). Incongruent ontogenetic maturity indicators in a Late Triassic archosaur (Aetosauria: *Typothorax coccinarum*). *The Anatomical Record*, 1–17. https://doi.org/10.1002/ar.25343